Articles

Decorating Conjugated Polymer Chains with Naturally Occurring Molecules: Synthesis, Solvatochromism, Chain Helicity, and Biological Activity of Sugar-Containing Poly(phenylacetylene)s

Kevin K. L. Cheuk,[†] Jacky W. Y. Lam,[†] Bing Shi Li,[†] Yong Xie,[‡] and Ben Zhong Tang*[,†,§]

Department of Chemistry and Department of Biology, The Hong Kong University of Science & Technology (HKUST), Clear Water Bay, Kowloon, Hong Kong, China, and Department of Polymer Science and Engineering, Zhejiang University, Hangzhou 310027, China

Received November 15, 2006; Revised Manuscript Received February 22, 2007

ABSTRACT: Phenylacetylene derivatives containing different sugar moieties and functional bridges (**1**−**5**) are synthesized. Their polymerizations are affected by organorhodium complexes, producing corresponding polymers P**1**−P**5** with high molecular weights (M_w up to 1.2×10^6) and stereoregularities (*Z* content up to 100%) in high yields (up to 99%). The polyene backbones undergo irreversible *Z*-to-*E* isomerization at ∼160−230 °C. The solutions of the polymers exhibit solvatochromism: their backbone absorptions change with variations in the surrounding media. The polymers show Cotton effects in the long wavelength region where their polyene backbones absorb, revealing that the chiral sugar pendants have induced the polymer chain to take a helical conformation with an excess in one-handedness. Inserting a flexible methylene spacer between the chiral pendant and the polyene backbone hampers the helicity induction process and lowers the backbone circular dichroism. The acetonide protection groups in most of the polymers can be selectively deprotected by acid-catalyzed hydrolysis, yielding polymers with "free" sugar appendages. The polymers are cytophilic and can stimulate the growth of living cells.

Introduction

Synthesis of helical polymers, especially their π-conjugated forms, is a topic of current interest.[1−3] It is envisioned that attaching bulky pendants of natural origin to a polymer chain with extended electronic conjugation will generate a "molecular wire" wrapped in a biocompatible sheath that are electrically conductive, photonically susceptible, and biologically active. Such polymers may find an array of high-tech applications as, for example, artificial neurons in smart biorobotics, synthetic muscles in intelligent devices, scaffold matrixes in tissue engineering, photoresponsive antennas in photosynthesis cells, and modulating units in controlled drug deliver systems,[4] in addition to their potential uses as asymmetric electrodes in electrochemical processes, light polarizing films in optical displays, and chiral stationary phases in chromatographic enantioseparation.

Polyacetylene is a symmetric chain of conjugated polymer.[5] The chain symmetry can be broken by attaching asymmetric pendant groups to the polyene backbone, inducing the polymer chain to rotate in a helical fashion.[6,7] We have been interested in the development of new biomimetic polymers through molecular functionalization of polyacetylene.[8] By incorporating naturally occurring molecular species into the conjugated polymer structure, we have succeeded in the synthesis of a number of new polymers consisting of polyacetylene backbone and amino acid and nucleoside pendants.[8,9] The chiral pendants confer helical conformation on the polyene backbone, and the chain amphiphilicity enables the polymers to assemble into a variety of biomimetic nanostructures such as micelles, vesicles, globules, and helical cables.[8]

Sugars are also naturally occurring molecules. Derivatives of sugars, especially their oligomers and polymers as well as their bioconjugates and modifications, are everywhere in the living systems and are particularly abundant on the membrane surfaces. Polysaccharides, for example, form a sugar coat or a "glycocalyx" on the cellular surface. It performs many biological functions, such as protecting plasma membrane from injuries, enabling immune system to selectively attack foreign organisms and cancerous cells, forming the basis for compatibility of blood transfusions, tissue grafts, and organ transplants, binding cells together to prevent tissues from falling apart, enabling sperm to recognize and bind to eggs, and guiding embryonic cells to their destinations in the body. On the basis of the "like likes like" principle, a polymer chain with a sugar coat or a "sweet husk" may well be biocompatible and may even stimulate the growth of living cells due to its cytophilic nature.

Attracted by the perspective, in this work, we worked on integrating sugar moieties into polyacetylene structure at the molecular level. Sugar-containing polyacetylenes have rarely

* Corresponding author: Ph +852-2358-7375; Fax +852-2358-1594; e-mail tangbenz@ust.hk.
[†] Department of Chemistry, HKUST.
[‡] Department of Biology, HKUST.
[§] Zhejiang University.

10.1021/ma062629d CCC: $37.00
Published on Web 03/21/2007

Chart 1

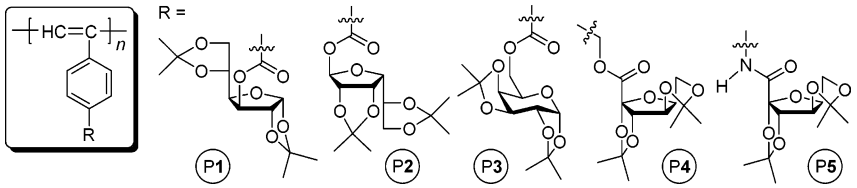

Scheme 1

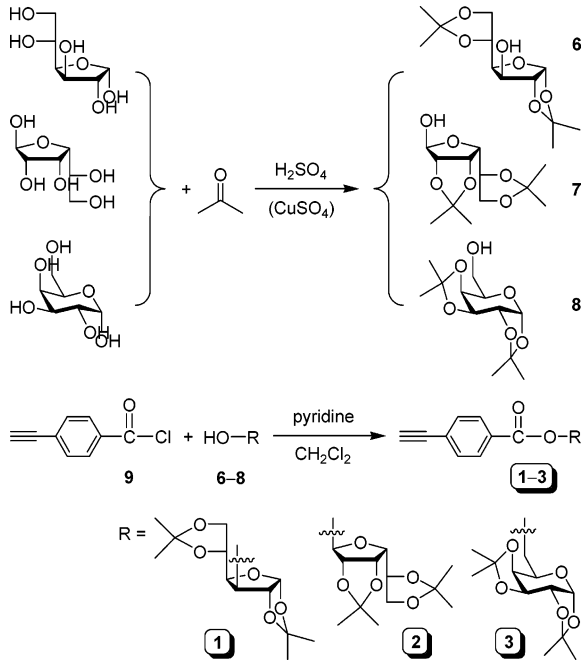

Scheme 2

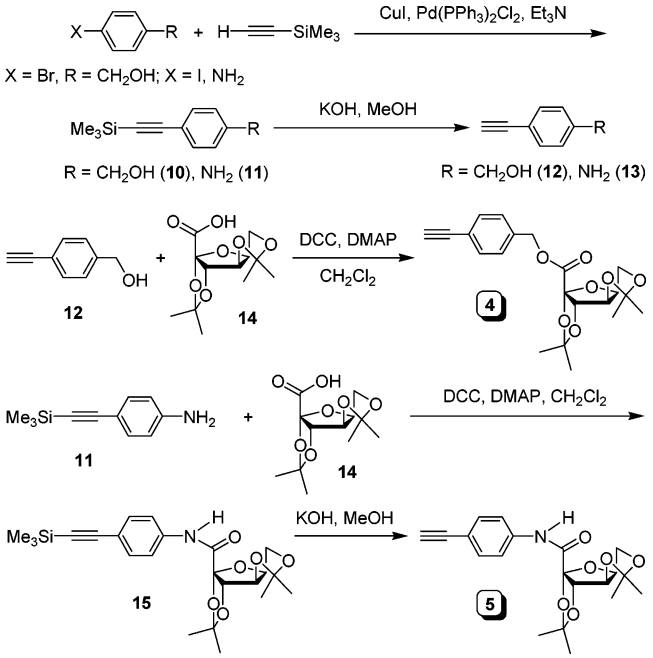

been prepared because of the synthetic difficulty associated with the multiple hydroxyl groups in a sugar molecule, whose acidic protons are poisoning to the transition-metal catalysts for acetylene polymerization.[8,10] In this paper, we report our effort in the synthesis of poly(phenylacetylene)s carrying sugar pendants (P**1**−P**5**; Chart 1). Taking a protection-chemistry approach, a number of phenylacetylene derivatives containing protected forms of monosaccharides including α-D-glucofuranose (or glucose), α-D-mannofuranose (or mannose), D-galactopyranose (or galactose), and L-gulonic acid (**1**−**5**) were synthesized (Schemes 1 and 2). The monomers were readily polymerized into high molecular weight polymers in high yields. The polymers take helical conformations and show, as expected, excellent biocompatibility.

Experimental Section

Full experimental details about the syntheses of the monomers and polymers (including the polyketal hydrolysis) and their spectroscopic analysis data are given in the Supporting Information.[11] The degree of hydrolysis (DH) of a polymer after the acid-catalyzed ketal hydrolysis was calculated from its ^{1}H NMR spectral data according to the following equation:

$$\mathrm{DH}\ (\%) = [1 - (A_{\mathrm{Me}}/12)/(A_{\mathrm{Ar+Vi}}/5)] \times 100\% \qquad (1)$$

where A_{Me} is the integral of the resonance of protons of the methyl groups remaining in the hydrolyzed polymer and $A_{\mathrm{Ar+Vi}}$ is the integral of the resonance of its aromatic and vinyl protons.

Results and Discussion

Monomer Synthesis. We designed phenylacetylene derivatives containing different monosaccharide moieties and elaborated multistep reaction routes for their synthesis. Because the hydroxyl groups in D-glucose, D-mannose, and D-galactose are toxic to the catalysts used for acetylene polymerizations, we first protected most of their OH groups by ketal formation with acetone. The resulting monohydroxyl products (**6**−**8**) are then reacted with 4-ethynylbenzoyl chloride, furnishing the desirable monomers **1**−**3** in satisfactory yields (Scheme 1).

We also prepared monomers **4** and **5**, which have different functional bridge groups, according to the synthetic pathways shown in Scheme 2. While **4** is readily accessible by esterification of 2,3:4,4-di-*O*-isopropylidene-2-keto-L-gulonic acid (**14**) with 4-ethynylbenzyl alcohol (**12**), an attempt to prepare **5** from direct reaction of **14** and 4-ethynylamide (**13**) by the same synthetic route failed. We thus reacted **14** with 4-(trimethylsilylethynyl)aniline (**11**) first and then cleaved the trimethylsilyl group in **15** in alcoholic KOH solution, which gave **5** in ∼86% yield. All the monomers were fully characterized by standard spectroscopic methods, from which satisfactory analysis data corresponding to their expected molecular structures were obtained (see Supporting Information for details).

Polymerization Reactions. We first tried to polymerize the monomers by tungsten and molybdenum halides, which are well-known catalysts for the polymerizations of substituted acetylenes.[8,12] Stirring THF solutions of **1** in the presence of WCl_6 or $MoCl_5$ with or without Ph_4Sn for extended periods of time produced, however, no polymeric products. Raising the temperature and changing the solvent both ended up yielding no polymers. The poisoning interactions of the polar functional sugar pendants with the early-transition-metal catalysts may have been responsible for the failure in the polymerization reactions.

Late-transition-metal catalysts such as $[Rh(nbd)Cl]_2$ and $[Rh(cod)Cl]_2$ (where nbd = 2,5-norborndiene and cod = 1,5-cyclooctadiene) are known to be more tolerant of functional

Table 1. Polymerization of 1,2:5,6-Di-*O*-isopropylidene-3-*O*-(4-ethynylbenzonyl)-α-D-glucofuranose (1)[a]

no.	catalyst	solvent[b]	yield (%)	M_w[c]	M_w/M_n[c]	*Z* (%)[d]
1	$[Rh(nbd)Cl]_2$	THF	82.3	734 000	16.1	98.7
2	$[Rh(nbd)Cl]_2$	THF/Et_3N	93.0	604 000	8.9	89.2
3	$[Rh(nbd)Cl]_2$	DCM	92.3	500 000	12.4	87.0
4	$[Rh(nbd)Cl]_2$	toluene	93.8	995 000	45.3	80.0
5	$Rh(nbd)(tos)(H_2O)$	THF	72.2	107 000	10.1	73.6
6	[Rh(cod)Cl]2	THF	77.5	556 000	17.1	86.3
7	$[Rh(cod)Cl]_2$	THF/Et_3N	85.4	342 000	7.9	77.8
8	$[Rh(cod)Cl]_2$	DCM	81.1	928 000	22.8	82.5
9	$Rh(cod)(NH_3)Cl$	THF	95.5	240 000	12.0	75.2
10	$Rh(cod)(tos)(H_2O)$	THF	55.7	501 000	9.4	86.9

[a] Carried out at room temperature under nitrogen for 24 h; $[monomer]_0 = 0.1$ M, [catalyst] = 5 mM. Abbreviations: nbd = 2,5-norborndiene, cod = 1,5-cyclooctadiene, tos = 4-toluenesulfonate, THF = tetrahydrofuran, DCM = dichloromethane. [b] Volume of solvent used: 2 mL; volume of Et_3N added: 1 drop. [c] Estimated by GPC in THF on the basis of a polystyrene calibration. [d] Determined by ^1H NMR analysis.

Table 2. Polymerization of 2,3:5,6-Di-*O*-isopropylidene-1-*O*-(4-ethynylbenzonyl)-α-D-mannofuranose (2)[a]

no.	catalyst	solvent	yield (%)	M_w	M_w/M_n	*Z* (%)
1	$[Rh(nbd)Cl]_2$	THF	93.8	547 000	8.0	93.9
2	$[Rh(nbd)Cl]_2$	THF/Et_3N	99.4	776 000	5.8	98.4
3	$[Rh(nbd)Cl]_2$	DCM	91.5	506 000	4.3	92.6
4	$[Rh(nbd)Cl]_2$	DCM/Et_3N	96.5	785 000	6.2	96.6
5	$[Rh(nbd)Cl]_2$	dioxane	72.3	282 000	6.7	99.2
6	$[Rh(nbd)Cl]_2$	toluene	91.1	433 000	4.6	83.3
7	$Rh(nbd)(tos)(H_2O)$	THF	trace			
8	$[Rh(cod)Cl]_2$	THF	68.5	287 000	8.3	85.6
9	$[Rh(cod)Cl]_2$	THF/Et_3N	86.6	1 074 000	8.1	97.8
10	$[Rh(cod)Cl]_2$	DCM	13.4	220 000	9.6	93.9
11	$[Rh(cod)Cl]_2$	DCM/Et_3N	99.5	770 300	5.6	99.5
12	$Rh(cod)(NH_3)Cl$	THF	87.8	181 000	7.1	88.6
13	$Rh(cod)(tos)(H_2O)$	THF	48.1	88 000	2.3	95.9

[a] See the footnotes given in Table 1 for the experimental conditions, measurement methods, and abbreviation definitions.

Table 3. Polymerization of 1,2:3,4-Di-*O*-isopropylidene-6-*O*-(4-ethynylbenzonyl)-D-galactopyranose (3)[a]

no.	catalyst	solvent	yield (%)	M_w	M_w/M_n	*Z* (%)
1	$[Rh(nbd)Cl]_2$	THF	89.0	718 000	15.7	98.9
2	$[Rh(nbd)Cl]_2$	THF/Et_3N	93.5	803 000	5.9	96.0
3	$[Rh(nbd)Cl]_2$	DCM	88.6	365 000	9.0	99.2
4	$[Rh(nbd)Cl]_2$	toluene	87.0	662 000	4.5	99.0
5	$Rh(nbd)(tos)(H_2O)$	THF	64.1	86 000	5.4	98.5
6	$[Rh(cod)Cl]_2$	THF	71.6	571 000	17.2	97.6
7	$[Rh(cod)Cl]_2$	THF/Et_3N	83.6	343 000	4.6	99.8
8	$[Rh(cod)Cl]_2$	DCM	71.7	1 236 000	34.9	96.2
9	$Rh(cod)(NH_3)Cl$	THF	88.6	361 000	5.8	94.4
10	$Rh(cod)(tos)(H_2O)$	THF	55.7	450 000	6.2	93.7

[a] See the footnotes given in Table 1 for the experimental conditions, measurement methods, and abbreviation definitions.

groups. We thus admixed **1** with a catalytic amount of $[Rh(nbd)Cl]_2$ in THF. Delightfully, after stirring at room temperature for 24 h, we obtained a high molecular weight polymer in a high yield (Table 1, no. 1). The polymer yield increases in the presence of Et_3N, but the molecular weight of the polymer decreased. Satisfactory polymerization results are also obtained in DCM and toluene solutions. Changing the rhodium catalyst to $Rh(nbd)(tos)(H_2O)$ gives, however, poorer results, implying that the catalytic activity of the rhodium complex is ligand-sensitive.

We further check the activity of other Rh complexes with different ligands. $[Rh(cod)Cl]_2$ works well for the polymerization in THF, furnishing a polymer with an M_w of $\sim 5.6 \times 10^5$ in ~78% yield (Table 1, no. 6). Similar to the case of $[Rh(nbd)Cl]_2$, addition of a small amount of Et_3N into the THF solution improves the polymer yield at the expense of the molecular weight. DCM is a good solvent for the polymerization: the reaction conducted in this solvent gives a polymer with a molecular weight 1.7-fold higher than that prepared in THF. $Rh(cod)(NH_3)Cl$ and $Rh(cod)(tos)(H_2O)$ complexes are also active for the acetylene polymerization, producing polymers with high molecular weights in ~96 and ~56% yields, respectively.

We then studied the polymerization of **2**, a phenylacetylene derivative containing a D-mannose moiety. Whereas the monomer undergoes sluggish polymerization reaction in the presence of WCl_6 or $MoCl_5$, high molecular weight polymers are obtained in high yields when the polymerization is catalyzed by $[Rh(nbd)Cl]_2$ (Table 2, no. 1). Among the monophasic solvents, the reaction carried out in THF produces a polymer with the highest M_w ($\sim 5.5 \times 10^5$) in ~94% yield. The polymerization results are even better when a small amount of Et_3N is added. Surprisingly, $Rh(nbd)(tos)(H_2O)$ shows almost no catalytic activity. The polymerization of **2** can also be affected by $[Rh(cod)Cl]_2$. The catalyst performs better in the solvents mixed with Et_3N. For example, the polymer yield and molecular weight obtained in DCM/Et_3N are respectively 7- and 3.5-fold higher than those prepared in DCM. $Rh(cod)(NH_3)Cl$ and $Rh(cod)(tos)(H_2O)$ are active in polymerizing **2**, but the results are generally poorer than those obtained from $[Rh(cod)Cl]_2$.

Table 3 summarizes the polymerization results for monomer **3**. All the organorhodium complexes catalyze the polymerization reactions well and produce high molecular weight polymers in high yields. The performance of $[Rh(nbd)Cl]_2$ is better than $Rh(nbd)(tos)(H_2O)$ and its derivatives containing a cod ligand. The

Table 4. Polymerization of 4-(2,3:4,6-Di-*O*-isopropylidene-2-keto-L-gulonoyloxymethyl)phenylacetylene (4)[a]

no.	catalyst	solvent	yield (%)	M_w	M_w/M_n	*Z* (%)
1	$[Rh(nbd)Cl]_2$	THF	41.0	88 000	4.0	89.4
2	$[Rh(nbd)Cl]_2$	THF/Et_3N	75.4	161 000	6.6	99.0
3	$[Rh(nbd)Cl]_2$	DCM	42.2	78 000	3.6	88.4
4	$[Rh(nbd)Cl]_2$	DCM/Et_3N	48.5	35 000	2.5	93.3
5	$[Rh(nbd)Cl]_2$	dioxane	54.4	98 000	6.4	94.2
6	$[Rh(nbd)Cl]_2$	toluene	trace			
7	$Rh(nbd)(tos)(H_2O)$	THF	40.5	19 000	4.4	94.7
8	$[Rh(cod)Cl]_2$	THF	trace			
9	$[Rh(cod)Cl]_2$	THF/Et_3N	25.6	45 000	3.7	86.5
10	$[Rh(cod)Cl]_2$	DCM	trace			
11	$[Rh(cod)Cl]_2$	DCM/Et_3N	51.0	42 000	3.3	91.7
12	$Rh(cod)(NH_3)Cl$	THF	48.8	52 000	4.1	91.0
13	$Rh(cod)(tos)(H_2O)$	THF	44.1	17 000	3.9	96.9

[a] See the footnotes given in Table 1 for the experimental conditions, measurement methods, and abbreviation definitions.

Table 5. Polymerization of 4-(2,3:4,6-Di-*O*-isopropylidene-2-keto-L-gulonoylamino)phenylacetylene (5)[a]

no.	catalyst	solvent	yield (%)	M_w	M_w/M_n	*Z* (%)
1	$[Rh(nbd)Cl]_2$	THF	47.3	26 000	2.2	87.5
2	$[Rh(nbd)Cl]_2$	THF/Et_3N	70.7	32 700	3.1	93.4
3	$[Rh(nbd)Cl]_2$	DCM	15.1	13 900	1.9	59.7
4	$[Rh(nbd)Cl]_2$	DCM/Et_3N	64.1	35 200	2.7	85.7
5	$[Rh(nbd)Cl]_2$	dioxane	50.8	31 800	2.2	89.3
6	$[Rh(nbd)Cl]_2$	toluene	64.7	32 700	3.3	65.4
7	$Rh(nbd)(tos)(H_2O)$	THF	trace			
8	$[Rh(cod)Cl]_2$	THF	trace			
9	$[Rh(cod)Cl]_2$	THF/Et_3N	23.5	107 500	2.5	90.4
10	$[Rh(cod)Cl]_2$	DCM	trace			
11	$[Rh(cod)Cl]_2$	DCM/Et_3N	43.6	223 600	2.8	88.5
12	$Rh(cod)(NH_3)Cl$	THF	33.5	24 400	2.4	80.4
13	$Rh(cod)(tos)(H_2O)$	THF	trace			

[a] See the footnotes given in Table 1 for the experimental conditions, measurement methods, and abbreviation definitions.

reaction conducted in THF/Et_3N gives a polymer with an M_w as high as $\sim 8.0 \times 10^5$ in ~94% yield (Table 3, no. 2).

The polymerizations of **4** carried out under the similar experimental conditions as given in Tables 1−3 produce polymers with lower molecular weights in lower yields (Table 4). Why the polymerization behavior of **4** is so different from those of **1**−**3** is unclear at present but may be related to the difference in the electron densities of their triple bonds. Because of the electron-withdrawing effect of the carbonyl group (−CO−) at the *p*-position of the phenyl ring, the ethynyl groups of **1**−**3** are electron-deficient, whereas that of **4** is electron-rich due to the electron-donating effect of the methoxy ($-CH_2O-$) group at the same position. The high electron density of the triple bond may have made **4** less reactive because electron-rich acetylene monomers generally possess lower polymerizability than their electron-poor counterparts.[13] This is further manifested by the polymerization results of **5** given in Table 5, which are similar to the inferior results obtained from the Rh-catalyzed polymerizations of the phenylacetylene derivatives containing *p*-amino groups (−NH−).[9d]

As can be seen from Table 5, not all the organorhodium complexes are capable of polymerizing **5**. Only are moderate results obtained when the polymerization reactions are catalyzed by $[Rh(nbd)Cl]_2$ and $[Rh(cod)Cl]_2$. Like in **4**, the catalysts work better in the solvent mixtures with Et_3N, furnishing polymers with higher molecular weights in higher yields.

Structural Characterization. The polymers are characterized by spectroscopic techniques, and all of them give satisfactory analysis data corresponding to their molecular structures. The monomers exhibit ≡C−H and C≡C stretching vibrations at ~3270 and ~2110 cm^{-1}, respectively, which are absent in the IR spectra of the polymers. The polymers exhibit no peaks associated with the resonances of the ethynyl protons at $\delta \sim$ 3.2 in their ^1H NMR spectra (Figure 1). New peaks are seen at $\delta \sim 5.8$, which correspond to the resonances of the olefin protons of the *Z*-*s*-*E* conformation of the polymers. Using an equation developed by our and other groups,[13−15] the *Z* content of P**1** is calculated to be 89%. Other polymers are also *Z*-rich (cf. Tables 1−5), agreeing with the early finding that the organorhodium complexes produce polyacetylenes with *Z*-rich conformations.[16] The resonance peaks of P**5** are much broader than those of P**1**−P**4**. This is not surprising, taking into the account that the amide functional groups are capable of forming hydrogen bonds. Formation of intra- and interstrand hydrogen bonds may have considerably stiffened the polyene chains and restricted their movements, hence broadening the resonance peaks of the polymer.[17]

Analyses by ^{13}C NMR spectroscopy also confirm that the acetylenic triple bonds of the monomers have been converted to the olefinic double bonds of the polymers. None of the polymers exhibits resonance peaks of the ethynyl carbons at δ 82.0 and 80.0. On the other hand, new peaks corresponding to the resonances of the backbone olefin carbons are observed at δ 145.0 and 128.0.

Thermal Properties. All the polymers are soluble in common organic solvents such as chloroform, DCM, dimethylforamide (DMF), and dimethyl sulfoxide (DMSO). The polymers are also thermally stable. Thermogravimetric analysis (TGA) reveals that P**1** does not lose any weight when it is heated to a temperature as high as ~280 °C (Figure 2). Polymers P**2**−P**4** decompose at similar temperatures, whereas P**5** exhibits a higher resistance to thermolysis. Hydrogen bonding may have rigidified the polymer chain, hence enhancing its thermal stability.

It is known that (unsubstituted) polyacetylene undergoes irreversible *Z*−*E* isomerization upon thermal treatment.[18] Since P**1**−P**5** are polyacetylene derivatives, their chain segments with

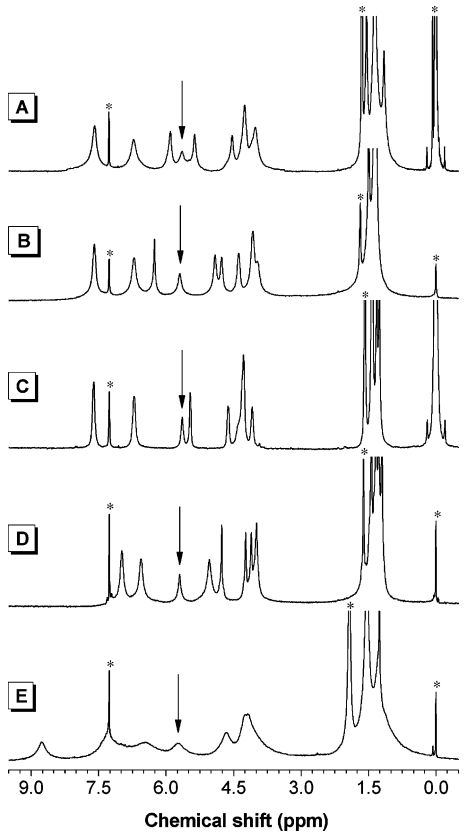

Figure 1. ^{1}H NMR spectra of chloroform-*d* solutions of (A) P**1** (sample taken from Table 1, no. 2), (B) P**2** (Table 2, no. 2), (C) P**3** (Table 3, no. 2), (D) P**4** (Table 4, no. 2), and (E) P**5** (Table 5, no. 2). The resonance peaks of the olefinic protons (═C−H) are marked with arrows, while those of TMS, solvents, and water are marked with asterisks.

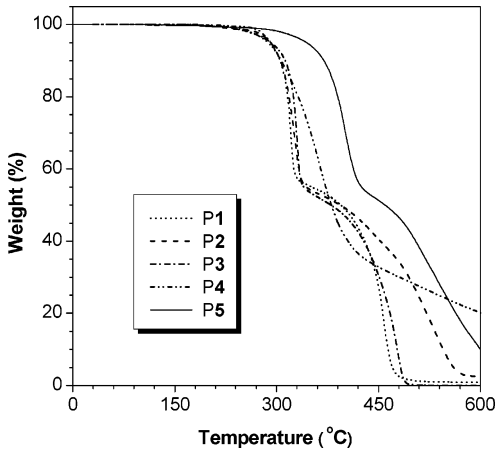

Figure 2. TGA thermograms of P**1** (sample from Table 1, no. 2), P**2** (Table 2, no. 2), P**3** (Table 3, no. 2), P**4** (Table 4, no. 2), and P**5** (Table 5, no. 2) measured under nitrogen at a heating rate of 20 °C/min.

Z conformation may also isomerize into *E* conformation when a sufficient amount of energy is supplied. Figure 3A shows the differential scanning calorimetry (DSC) curves of P**5**. In the first heating scan, P**5** starts to evolve an exothermic valley from ∼230 °C. Since P**5** is thermally stable below ∼350 °C (cf. Figure 2), the exothermic valley bottomed at ∼245 °C should be associated with its thermal *Z*-to-*E* isomerization. Like that of its polyacetylene parent, the isomerization process of P**5** is irreversible: the successive first cooling and second heating scans detect no any peaks at ∼245 °C, giving almost flat lines parallel to the abscissa over the whole scanned temperature region. No glass transition is observed, possibly because it occurs beyond the scanned temperature region, noticing that substituted polyacetylenes often show very high glass transition temperatures due to the rigidity of their polyacetylene backbones.[18b] Other polymers exhibit similar DSC thermograms, but their exothermic valleys appear at lower temperatures. These polymers contain no amide functional groups, and therefore no

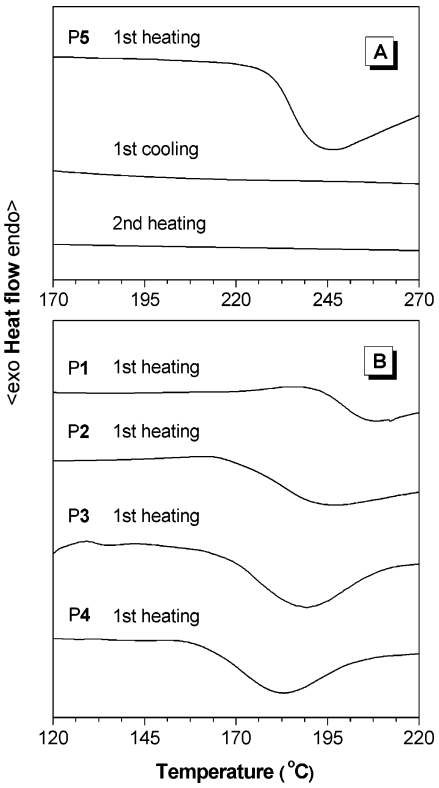

Figure 3. DSC thermograms of (A) P**5** (sample taken from Table 5, no. 2) and (B) P**1** (Table 1, no. 2), P**2** (Table 2, no. 2), P**3** (Table 3, no. 2), and P**4** (Table 4, no. 2) recorded under nitrogen at a heating or cooling rate of 10 °C/min.

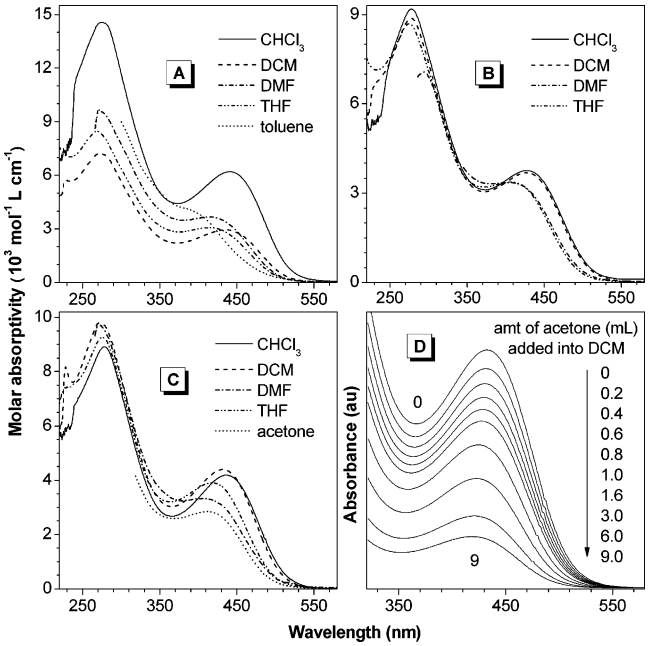

Figure 4. UV−vis absorption spectra of (A) P**1** (sample taken from Table 1, no. 2), (B) P**2** (Table 2, no. 2), and (C) P**3** (Table 3, no. 2) in different solvents. (D) Change of backbone absorption of P**3** with the addition of acetone into its DCM solution. Polymer concentration: ∼0.1−0.2 mM. The spectral data in DMF below 260 nm were not taken because of the interfering solvent absorption.

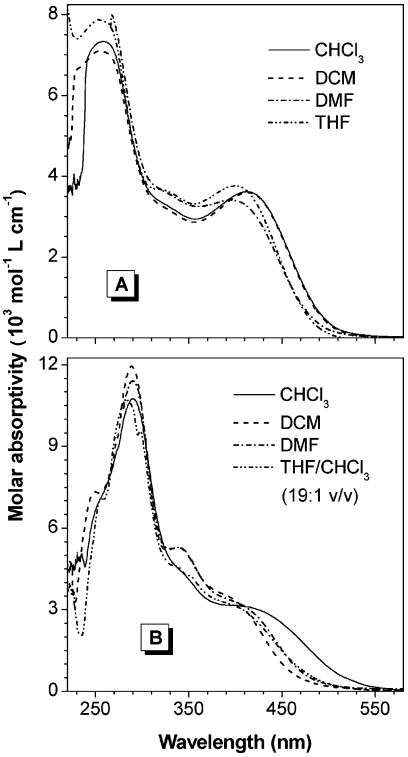

Figure 5. UV absorption spectra of (A) P**4** (sample taken from Table 4, no. 2) and (B) P**5** (Table 5, no. 2) in different solvents. Polymer concentration: ~0.1 mM. The spectral data in DMF below 260 nm were not taken because of the interfering solvent absorption.

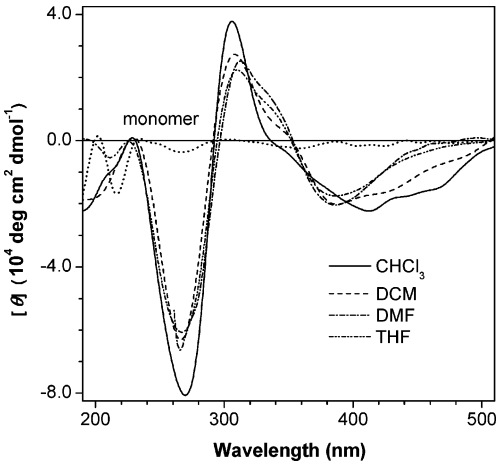

Figure 6. CD spectra of P**1** (sample taken from Table 1, no. 2) in different solvents. Polymer concentration: ~1 mM. The CD spectrum of a chloroform solution of its monomer (**1**) with a similar concentration is shown for comparison. The spectra data in DMF below 260 nm are not taken because of the interfering solvent absorption.

additional energy is needed to break the strong hydrogen bonds.

Solvatochromism. Polymers P**1**−P**5** are amphiphilic, possessing hydrophobic polyene backbones and hydrophilic sugar appendages. The polymer chains may thus take different conformations in the solvents with different polarities and solvating powers and undergo different electronic transitions. This is indeed the case: the polymers exhibit solvatochromism, with their absorption spectra changed with solvents of their solutions.[19]

Figure 4A shows the UV−vis absorption spectra of P**1** in different solvents. In chloroform, its polyene backbone absorbs strongly at ~450 nm. When the solvent is changed to DCM, DMF, and then THF, the absorption becomes weaker and shifts

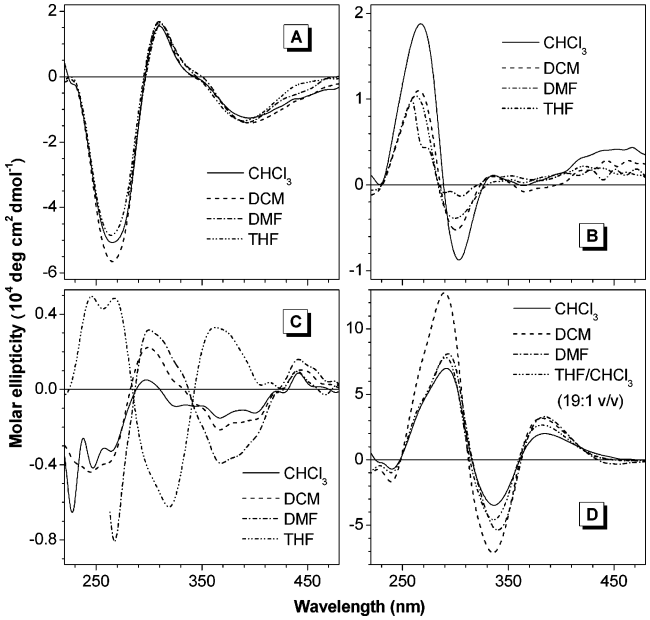

Figure 7. CD spectra of (A) P**2** (sample taken from Table 2, no. 2), (B) P**3** (Table 3, no. 2), (C) P**4** (Table 4, no. 2), and (D) P**5** (Table 5, no. 2) in different solvents. Polymer concentration: ~1 mM. The spectral data in DMF below 260 nm are not taken because of the interfering solvent absorption.

progressively to shorter wavelengths. Further weakening and blue shift are observed when the spectrum is measured in toluene. The solvatochromism is probably caused by the conformational change in the solvents. Chloroform is a good solvent with high solvating power to both the hydrophobic

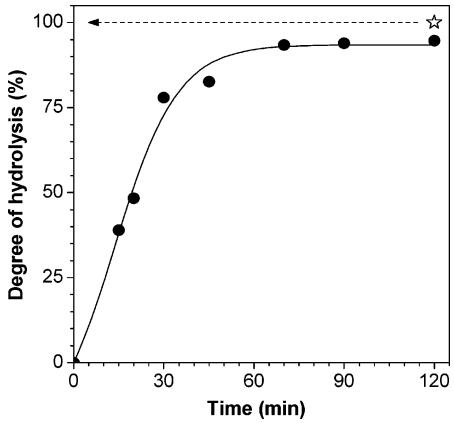

Figure 8. Change in the degree of hydrolysis of P**3** with time in CF_3CO_2H/THF/H_2O mixtures (volume ratio: 7:2:1, solid circles; 9:2:1, open star). Reaction temperature: room temperature (~23 °C). Polymer concentration: ~50 mM.

backbone and hydrophilic pendants. The polymer strands may be well-solvated by the solvent molecules and take a well-extended planar conformation, in which the polyene backbone is better conjugated. Toluene is, however, a poor solvent of the hydrophilic appendages. To minimize their exposure to the unfavorable environment, the sugar pendants may aggregate together. Under such circumstances, the polymer chain may take a coiled, nonplanar conformation, leading to a reduction in the effective conjugation length of the polyene backbone.

The UV spectra of P**2** resemble those of P**1** but with lower absorptivity (Figure 4B). In chloroform and DCM, the backbone absorbs at 440 nm. When the measurements are taken in THF and DMF, the absorption peak blue-shifts to 420 nm. Polymer P**3** shows the longest and highest backbone absorptions in

Table 6. Specific Rotations of Sugar-Containing Phenylacetylene Derivatives and Their Polymers in Different Solvents

	$[\alpha]_D^{23}$, deg (*c*, g/dL)									
solvent	**1**	P**1**	**2**	P**2**	**3**	P**3**	**4**	P**4**	**5**	P**5**
chloroform	−96.8 (3.523)	−874.2 (0.072)	−49.4 (1.490)	−515.4 (0.039)	−40.8 (5.000)	+219.7 (0.049)	−10.2 (0.960)	−31.0 (0.045)	+30.2 (1.950)	+535.6 (0.045)
DCM		−637.1 (0.103)		−507.3 (0.041)		+98.3 (0.058)		−42.9 (0.042)		+556.4 (0.039)
DMF		−560.3 (0.058)		−353.1 (0.032)		+24.4 (0.041)		−53.5 (0.043)		+495.6 (0.045)
THF	−53.4 (0.272)	−498.6 (0.071)		−334.0 (0.047)	−37.0 (0.338)	+64.3 (0.089)		+33.3 (0.042)		+462.5[a] (0.040)
dioxane		−447.9 (0.040)				+59.6 (0.053)				
acetone		−428.9 (0.099)				+29.8 (0.066)				
toluene	−97.2 (0.311)	−264.3 (0.030)			−29.8 (0.506)	+10.3 (0.128)				
acetonitrile	−50.0 (0.298)				−34.5 (0.650)	+42.9 (0.062)				

[a] Measured in THF/chloroform (19:1 by volume).

chloroform and DCM. The peak maximum does not change much in THF, DMF, and acetone, but the absorptivity decreases. Varying the composition of the DCM/acetone mixture changes the UV spectrum in a continuous and reversible fashion (Figure 4D). It is understandable because the conformational change involves only noncovalent solvent−polymer interaction.

The backbone absorption of P**4** is peaked at 420 nm in chloroform and DCM (Figure 5A). The peak shifts to 400 nm in THF and DMF. Polymer P**5** in chloroform exhibits backbone absorptions at 440 nm with the absorption edge well extending to 560 nm. When measured in DMF, THF/chloroform (P**5** is only partially soluble in pure THF), and then DCM, the spectrum shifts progressively to the low wavelength region.

Chain Helicity. The bulky pendants of neighboring repeat units may not be able to locate on the same plane but twist an angle to avoid the involved steric crowdedness. When the appendages are chiral, their cooperative twisting toward a preferred direction may generate an asymmetric force field to induce the segments of a polymer chain to spiral in a helical fashion. To check whether the bulky, chiral sugar pendants would induce the chains of P**1**−P**5** to helically rotate, we measured their specific optical rotations ($[\alpha]_D^{23}$) in different solvents. The $[\alpha]_D^{23}$ values of P**1** and P**2** are much higher than their monomers in the same solvents (Table 6). These high optical activities suggest that the polymer strands of P**1** and P**2** are taking helical conformations with an excesses of preferred handedness.[20] The magnitude but the sign of their $[\alpha]_D^{23}$ values changes with solvent. This is different from the amino acid-containing poly(phenylacetylene)s, whose specific optical rotations reverse their signs even when the polarities of the solvents are similar.[9b,c] Compared with amino acids, monosaccharides are bulkier and more rigid, and their rotation around the polymer backbone is thus sterically more demanding. This restricted motion of the pendants may have fixed the "natural" chain conformations to a large extent, thus making the polymer chain less responsive to the variation in its environmental surrounding.

Whereas the $[\alpha]_D^{23}$ values of monomer **3** are all negative, those of its polymer P**3** are opposite in sign, implying that the optical activity of the polymer is determined by the helicity of its polyene backbone. The $[\alpha]_D^{23}$ values of P**3** are all smaller than those of P**1** and P**2** in absolute terms, suggesting that the methylene bridge between the polyacetylene backbone and the monosaccharide pendants has hindered the chirality transcription process to some extent. Polymer P**4** also contains a methylene bridge, whose $|[\alpha]_D^{23}|$ values are even lower, once again suggesting that the flexible methylene linkage has impeded the transcription of the pendant chirality to the backbone helicity. When the flexible spacer is changed to a rigid amide bridge (−NHCO−) in P**5**, large $[\alpha]_D^{23}$ values are observed. This offers an opportunity to tune the optical activity of the polymers by molecular engineering endeavor.

The high $[\alpha]_D^{23}$ values of the polymers imply that their backbones are helically rotating. To confirm this, we conducted circular dichroism (CD) analysis, a powerful tool for studying helical structures.[21] Figure 6 shows the CD spectra of monomer **1** in chloroform and its polymer P**1** in different solvents. In chloroform, P**1** exhibits strong Cotton effects at 270, 300, and 390 nm. Since monomer **1** is practically CD-inactive at wavelengths >280 nm, the peaks in the long wavelength region thus should be associated with the absorption of the polyene backbone, thus unambiguously proving that the polymer chain adopts a helical conformation with a preferred screw sense. The spectral profile does not change much in DCM, DMF, and THF. The peak intensities are also similar, indicating that the helical conformation of the polymer is quite stable to solvent perturbation.

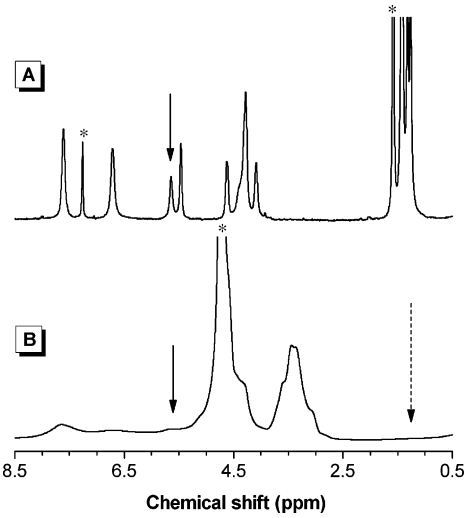

Figure 9. ^{1}H NMR spectra of (A) P**3** (sample taken from Table 3, no. 2) and (B) its hydrolyzed product P**3**h obtained after hydrolysis in CF_3CO_2H/THF/H_2O (9:2:1 by volume) for 2 h in (A) chloroform-*d* and (B) alkalified D_2O (KOH) solutions. The resonance peaks of the vinyl protons (═C−H) are marked with solid arrows, while those of the solvents and water are labeled with asterisks.

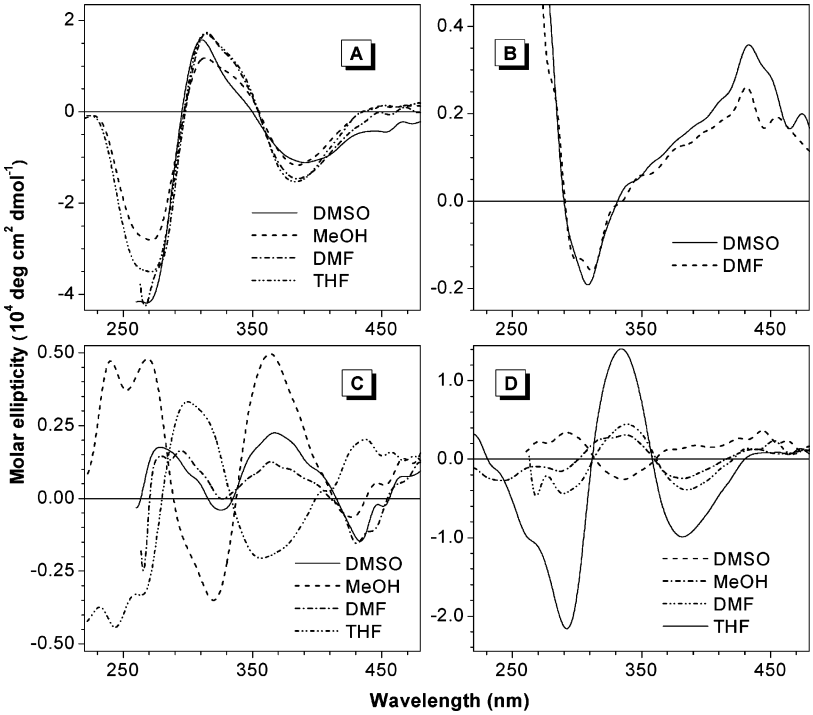

Figure 10. CD spectra of (A) P**1**h, (B) P**3**h, (C) P**4**h, and (D) P**5**h in different solvents. Polymer concentration: ~1 mM. The spectral data in DMSO and DMF below 260 nm are not taken because of the interfering solvent absorptions.

Polymer P**2** also exhibits strong backbone CD bands. In chloroform, its first Cotton effect is observed at ~400 nm with a molar ellipticity of about −14 000 deg cm^2 dmol^{-1} (Figure 7A). Like P**1**, its chain helicity changes little with solvent, and its CD spectra measured in DCM, DMF, and THF are all similar to that taken in chloroform. Unlike P**1** and P**2**, the first Cotton effect of P**3** is found at ~460 nm with a sign inversion in chloroform. The molar ellipticity is low, probably due to the flexible methylene spacer, which hinders the chiral transcription process from the sugar pendants to the polyacetylene backbone. Similar spectra with lower molar ellipticities are observed in DCM, DMF, and THF.

Since the chiral pendants of P**4** are also separated from its backbone by a methylene linkage group, its CD spectrum exhibits only weak backbone CD bands centered at ~380 nm in chloroform (Figure 7C). In DCM and DMF, the peak ellipticity becomes somewhat stronger. Interestingly, in THF, the sign of the CD spectrum of P**4** is completely reversed, indicating that the relative population of its left- and right-handed segments is switched. When the methylene groups in P**4** are changed to amide groups in P**5**, a strong CD band with a high molar ellipticity of ~23 000 deg cm^2 dmol^{-1} is observed at ~400 nm in chloroform. The CD band is intensified progressively when the solvent is changed to THF/chloroform, DCM, and then DMF. The amide groups may have facilitated the transcription of the pendant chirality to the backbone helicity. The helical conformation may have been stabilized by the formation of intra- and interstrand hydrogen bonds, resulting in the high backbone CD absorptions in P**5**.

Table 7. Acid-Catalyzed Decapping of the Monosaccharide Pendants of Poly(phenylacetylene)s[a]

no.	1	2	3	4	5
polymer	P**1**h	P**2**h	P**3**h	P**4**h	P**5**h
DH (%)[b]	63.1	c	39.0	43.7	54.6

[a] Carried out in a CF_3CO_2H/THF/H_2O mixture (7:2:1 by volume) at room temperature for 15 min. Polymer concentration: ~50 mM. [b] Degree of hydrolysis (DH) calculated from eq 1 using ^{1}H NMR spectral data. [c] A large portion of the D-mannose groups were cleaved by the acid-catalyzed hydrolysis reaction.

Ketal Hydrolysis. After studying the chiroptical properties of polymers P**1**−P**5**, we tried to cleave the protection groups of their sugar pendants. An aqueous solution of trifluoroacetic acid is known to be effective for ketal hydrolysis with minimum side reactions.[22] To determine whether our polymers can be hydrolyzed by such a solution, we studied the time course of hydrolysis of P**3**, using aqueous solutions with different acid concentrations. To enhance polymer solubility, we added certain amounts of THF into the mixtures. Figure 8 shows the change in the degree of hydrolysis (DH) of P**3** with time in a CF_3CO_2H/THF/H_2O mixture (7:2:1 by volume). The DH increases rapidly in the first 30 min and changes slowly afterward. The DH obtained in 70 min is ~90%. Even if we prolong the reaction time, the DH is hardly changed. On the other hand, if we used a more acidic solution (CF_3CO_2H/THF/H_2O = 9:2:1) for the hydrolysis, the DH can achieve 100% within 2 h.

The product obtained from the hydrolysis of P**3** in the CF_3CO_2H/THF/H_2O mixture (9:2:1 by volume) is characterized by ^{1}H NMR spectroscopy. The methyl groups of P**3** resonate at δ 1.44, 1.33, and 1.27, which completely disappear after the hydrolysis (Figure 9). The transformation of the acetonide groups to the hydroxyl groups after hydrolysis upfield-shifts the resonances of the sugar protons, which are now observed at $\delta \sim 3.5$. This suggests that the hydrolysis reaction has proceeded to completion and has caused no harm on the ester functional group. Because of the numerous hydroxyl groups and hence the hydrogen bond formation in the polymer, the hydrolyzed product is not soluble in common organic solvents. Even when it is dissolved in aqueous KOH solution, many of the hydrogen bonds in the polymer are still preserved, as manifested by its very broad NMR signals.

To enhance solubility, we prepared partially deprotected polymers by partial hydrolysis of P**1**−P**5** in a CF_3CO_2H/THF/H_2O mixture (7:2:1 by volume) for only 15 min. Except for P**2**, all the monosaccharide-containing polymers can undergo

Table 8. Specific Optical Rotations of Partially Deprotected Sugar-Containing Poly(phenylacetylene)s[a] in Different Solvents

	$[\alpha]_D^{23}$, deg (*c*, g/dL)			
solvent	P**1**h	P**3**h	P**4**h	P**5**h
DMSO	−583.3 (0.030)	+85.4 (0.041)	+8.6 (0.030)	+72.6 (0.051)
DMF	−324.4 (0.041)	+54.1 (0.061)	−7.7 (0.039)	−40.6 (0.032)
THF	−318.2 (0.033)		−32.6 (0.046)	−136.4 (0.033)
MeOH	−207.9 (0.038)		+33.3 (0.033)	+9.7 (0.031)

[a] Prepared by hydrolysis in a $CF_3CO_2H/THF/H_2O$ mixture (7:2:1 by volume) for ∼15 min.

selective deprotection via ketal hydrolysis. Their DH values are given in Table 7. Under the same conditions, the DH value of the hydrolyzed product P**1**h is higher than those of P**5**h, P**3**h, and P**4**h. Polymer P**2** is an outstanding exception, whose ester bonds are also hydrolyzed when we tried to remove the acetonide groups. Because of the presence of the free sugar moieties, polymers P**1**h, P**3**h, and P**5**h, unlike their parent forms (P**1**, P**3**, and P**5**), are insoluble in chloroform and toluene but can dissolve in polar solvents such as DMSO and DMF.

Figure 10A shows the CD spectra of P**1**h in different solvents. Strong Cotton effects are observed at 310 and 390 nm in DMSO where the polyene backbone absorbs, revealing that the polymer chains are still helically rotating. This is also supported by the large $[\alpha]_D^{23}$ value of the polymer in this solvent (Table 8). Like P**1**, the chain helicity of P**1**h changes little with solvents: the spectra measured in MeOH, DMF, and THF all resemble that in DMSO with similar or slightly higher molar ellipticities.

Similarly, P**3**h is also optically active and shows CD bands associated with the helicity of the polyene backbone at ∼430 nm in DMSO and DMF (Figure 10B). Unlike P**1**h and P**3**h, P**4**h exhibits chiroptical properties opposite to those of its parent form P**3**. The first Cotton effect is also observed at 380 nm in DMF, but the sign is opposite. The absorptivity becomes higher in DMSO and MeOH, with the value measured in MeOH being 5-fold higher than that in DMF. In THF, the spectrum is completely inverted, indicating that the polymer takes an opposite helical screw sense in this solvent.

The helical chain segments of P**5**h take a screw sense opposite to those of its parent form P**5** in the same solvents. In DMSO, only weak backbone CD bands peaked at 340 and 420 nm are observed. The absorptions become stronger in MeOH, accompanied by a sign inversion. The CD bands are further intensified when the measurements are done in DMF and THF.

The UV spectra of P**1**h and P**3**h−P**5**h are shown in Figure 11. Like its parent form P**1**, polymer P**1**h shows solvatochromism. In DMSO, the polyacetylene backbone absorbs at 430 nm. When the solvent is changed to DMF, THF, and then MeOH, the spectrum blue-shifts progressively, accompanied by lowering peak intensities. The absorption spectra of P**3**h−P**5**h do not change much with solvent. The hydrolyzed polymers are insoluble in nonpolar solvents, making it difficult to measure their spectra in solvents with appreciably different polarities.

Biological Activity. Wrapping the molecular wires of polyacetylene backbones with the pendants of naturally occurring building blocks is expected to impart biocompatibility to the conjugated polymers. To check whether our sugar-containing polyacetylenes are biocompatible, we studied the cytotoxicity of P**3** to living HeLa cells. The cells are subcultured onto the microtiter plates (without polymer coating), into which a THF solution of P**3** is added a few hours after the cells have been seeded. The cells are stained with trypan blue and counter with a hemocytometer. In the presence of a small amount of P**3**, the cells grow faster. At a concentration of ∼0.1 μg/mL, the cell population is 20-fold higher than that of the control, although

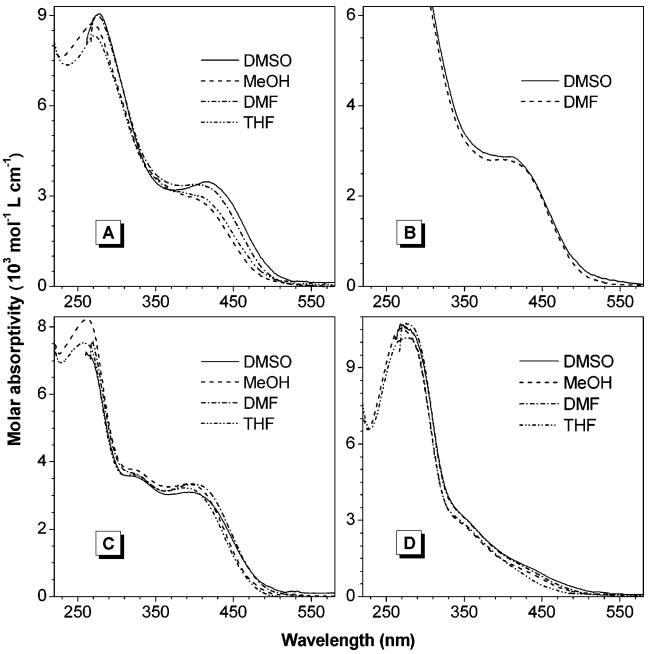

Figure 11. UV−vis absorption spectra of (A) P**1**h, (B) P**3**h, (C) P**4**h, and (D) P**5**h in different solvents. Polymer concentration: ∼0.1 mM. The spectral data in DMSO and DMF below 260 nm are not taken because of the interfering solvent absorption.

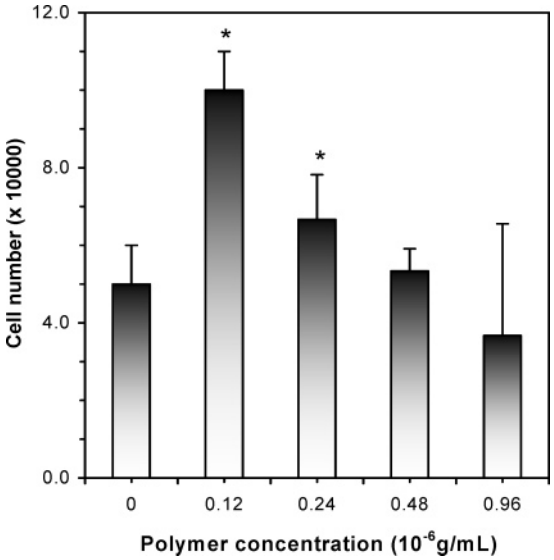

Figure 12. Influence of P**3** (sample taken from Table 3, no. 2) on the growth of HeLa cells at different concentrations after 3 days incubation.

the cell growth returns to normal when the polymer concentration becomes higher (Figure 12). This proves that the polymer is bioactive and cytocompatible. We have attempted to study the biological activity of P**3**h, but it is hindered by its limited solubility in common solvents.

Concluding Remarks

In this work, we have synthesized a group of phenylacetylene derivatives containing sugar moieties (**1**−**5**) and polymerized them into high molecular weight polymers (P**1**−P**5**) with high stereoregularities in high yields by the organorhodium catalysts. The chain conformations of the polymers can be readily isomerized by a simple process: heating them to ∼160−230 °C changes their *Z* conformers to *E* isomers. The polymers exhibit solvatochromism and their backbone absorptions change with the variations in the surrounding environment. All the

polymers show CD bands in the long wavelength region, confirming that the bulky, chiral sugar pendants have induced the polymer chains to spiral in a screw sense. Among the polymers, P**3** and P**4** show lower helicity because their flexible methylene spacers hamper the chiral transcription from of the sugar pendants to the polyene backbone. Except for P**2**, all other polymers can undergo selective deprotection reactions via ketal hydrolysis, yielding optically active polyacetylenes with completely or partially "free" monosaccharide appendages. The polymers are cytocompatible and can stimulate the growth of living cells, which may enable them to find an array of biotech applications in, e.g., tissue engineering, artificial nerves, and cytotech robotics.[23,24]

Acknowledgment. The work reported in this paper was partially supported by the Research Grants Council of Hong Kong (602706, HKU2/05C, 603505, and 603304), the National Science Foundation of China (20634020), and the Ministry of Science and Technology of China (2002CB613401). B.Z.T. thanks the support from Cao Guangbiao Foundation of Zhejiang University.

Supporting Information Available: Details for materials and instrumentations used in his study and experimental procedures for the monomer preparation, polymer synthesis, hydrolysis reaction, and cell incubation. This material is available free of charge via the Internet at http://pubs.acs.org.

References and Notes

(1) (a) Tang, H. Z.; Boyle, P. D.; Novak, B. M. *J. Am. Chem. Soc.* **2005**, *127*, 2136. (b) Ciferri, A. *Macromol. Rapid Commun.* **2002**, *23*, 511. (c) Yu, S. M.; Soto, C. M.; Tirrell, D. A. *J. Am. Chem. Soc.* **2000**, *122*, 6552. (d) Cha, J. N.; Stucky, G. D.; Morse, D. E.; Deming, T. J. *Nature (London)* **2000**, *403*, 289. (e) Chung, Y. I.; Christianson, L. A.; Stanger, H. E.; Powell, D. R.; Gellman, S. H. *J. Am. Chem. Soc.* **2000**, *120*, 10555. (f) Akagi, K.; Piao, G.; Kaneko, S.; Sakamaki, K.; Shirakawa, H.; Kyotani, M. *Science* **1998**, *282*, 1683.

(2) (a) Jenekhe, S. A.; Chen, X. I. *Science* **1999**, *283*, 372. (b) Lashuel, H. A.; LaBrenz, R.; Woo, L.; Serpell, L. C.; Kelly, J. W. *J. Am. Chem. Soc.* **2000**, *122*, 5262. (c) Zubarev, E. R.; Pralle, M. U.; Li, L. M.; Stupp, S. I. *Science* **1999**, *283*, 523. (d) Whitesides, G. M.; Ismagilov, R. F. *Science* **1999**, *284*, 89. (e) Rowan, A. E.; Nolte, R. J. M. *Angew. Chem., Int. Ed.* **1988**, 37. (f) James, T. D.; Shinkai, S. *Top. Curr. Chem.* **2002**, *218*, 159. (g) Cornelissen, J. J. L. M.; Rowan, A. E.; Nolte, R. J. M.; Sommerdijk, N. A. J. M. *Chem. Rev.* **2001**, *101*, 4039.

(3) (a) Yashima, E.; Maeda, K.; Okamoto, Y. *Nature (London)* **1999**, *399*, 449. (b) Nelson, J. C.; Saven, J. G.; Moore, J. S.; Wolynes, P. G. *Science* **1997**, *277*, 1793. (c) Rivera, J. M.; Craig, S. L.; Martin, T.; Rebek, J., Jr. *Angew. Chem., Int. Ed.* **2000**, *39*, 2130. (d) Green, M. M.; Cheon, K. S.; Yang, S. Y.; Park, J. W.; Swansburg, S.; Liu, W. H. *Acc. Chem. Res.* **2001**, *34*, 672. (e) Fujiki, M. *Macromol. Rapid Commun.* **2001**, *22*, 539. (f) Lawrence, D. S.; Jiang, T.; Levett, M. *Chem. Rev.* **1995**, *95*, 2229.

(4) (a) Yalpani, M. *Biomedical Functions and Biotechnology of Natural and Artifical Polymers*; ATL Press: Mount Prospect, IL, 1996. (b) Micolini, C. A. *Molecular Bioelectronics*; World Scientific: Hong Kong, 1996. (c) *Biomedical Materials−Drug Delivery, Implants, and Tissue Engineering*; Neenan, T., Marcolongo, M., Valentini, R. F., Eds.; MRS: Warrendale, PA, 1999.

(5) (a) Shirakawa, H. *Angew. Chem., Int. Ed.* **2001**, *40*, 2575. (b) MacDiarmid, A. G. *Angew. Chem., Int. Ed.* **2001**, *40*, 2581. (c) Heeger, A. J. *Angew. Chem., Int. Ed.* **2001**, *40*, 2591.

(6) (a) Ciardelli, F.; Lanzillo, S.; Pieroni, O. *Macromolecules* **1974**, *7*, 174. (b) Tang, B. Z.; Kotera, N. *Macromolecules* **1989**, *22*, 4388. (c) Masuda, T.; Sanda, F. In *Handbook of Metathesis*; Grubbs, R. H., Ed.; Wiley-VCH: Weinheim, 2003; Vol. 3, Chapter 3.11.

(7) (a) Lam, J. W. Y.; Dong, Y.; Cheuk, K. K. L.; Tang, B. Z. *Macromolecules* **2003**, *36*, 7927. (b) Zhao, H.; Sanda, F.; Masuda, T. *J. Polym. Sci., Part A: Polym. Chem.* **2005**, *43*, 5168. (c) Onouchi, H.; Hasegawa, T.; Kashiwagi, D.; Lshiguro, H.; Maeda, K.; Yashima, E. *Macromolecules* **2005**, *38*, 8625.

(8) (a) Lam, J, W. Y.; Tang, B. Z. *Acc. Chem. Res.* **2005**, *38*, 745. (b) Cheuk, K. K. L.; Li, B. S.; Tang, B. Z. In *Encyclopedia of Nanoscience and Nanotechnology*; Nalwa, H. S., Ed.; American Scientific Publishers: Stevenson Ranch, CA, 2004; Vol. 8, p 703. (c) Lai, L. M.; Lam, J. W. Y.; Qin, A.; Dong, Y.; Tang, B. Z. *J. Phys. Chem. B* **2006**, *110*, 11128.

(9) (a) Li, B.; Kang, S.; Cheuk, K. K. L.; Wan, L.; Ling, L.; Bai, C.; Tang, B. Z. *Langmuir* **2004**, *20*, 7589. (b) Cheuk, K. K. L.; Lam, J. W. Y.; Lai, L. M.; Dong, Y. P.; Tang, B. Z. *Macromolecules* **2003**, *36*, 9572. (c) Cheuk, K. K. L.; Lam, J. W. Y.; Chen, J.; Lai, L. M.; Tang, B. Z. *Macromolecules* **2003**, *36*, 5947. (d) Li, B.; Cheuk, K. K. L.; Salhi, F.; Lam, J. W. Y.; Cha, J. A. K.; Xiao, X.; Bai, C.; Tang, B. Z. *Nano Lett.* **2001**, *1*, 323.

(10) (a) Cheuk, K. K. L.; Lam, J. W. Y.; Sun, Q.; Cha, J. A. K.; Tang, B. Z. *Polym. Prepr.* **1999**, *40* (2), 655. (b) Yashima, E.; Maeda, K.; Sata, O. *J. Am. Chem. Soc.* **2001**, *123*, 8159. (c) Li, B. S.; Cheuk, K. K. L.; Zhou, J.; Xie, Y.; Cha, J. A. K.; Xiao, X.; Tang, B. Z. *Polym. Prepr.* **2001**, *42* (1), 543. (d) Kadokawa, J.-I.; Tawa, K.; Kaneko, Y.; Tabata, M. *Polym. Prepr.* **2005**, *46* (2), 1072.

(11) Tang, B. Z.; Poon, W. H.; Leung, S. M.; Leung, W. H.; Peng, H. *Macromolecules* **1997**, *30*, 2209 and references therein.

(12) (a) Masuda, T.; Higashimura, T. *Adv. Polym. Sci.* **1987**, *81*, 121. (b) Ginsburg, E. J.; Gorman, C. B.; Grubbs, R. H. In *Modern Acetylene Chemistry*; Stang, P. J., Diederich, F., Eds.; VCH: New York, 1995; Chapter 10, pp 353−383. (c) Lam, J. W. Y.; Kong, X.; Dong, Y. P.; Cheuk, K. K. L.; Xu, K.; Tang, B. Z. *Macromolecules* **2000**, *33*, 5027. (d) Tabata, M.; Stone, T.; Sadahiro, Y. *Macromol. Chem. Phys.* **1999**, *200*, 265. (e) Choi, S. K.; Gal, Y. S.; Jin, S. H.; Kim, H. K. *Chem. Rev.* **2000**, *100*, 1645.

(13) (a) Tang, B. Z.; Kong, X.; Wan, X.; Feng, X.-D. *Macromolecules* **1997**, *30*, 5620. (b) Lam, J. W. Y.; Tang, B. Z. *J. Polym. Sci., Part A: Polym. Chem.* **2003**, *41*, 2607. (c) Dong, H.; Zheng, R.; Lam, J. W. Y.; Häussler, M.; Tang, B. Z. *Macromolecules* **2005**, *38*, 6382. (d) Häussler, M.; Tang, B. Z. *Adv. Polym. Sci.*, in press.

(14) (a) Percec, V.; Rudick, J. G.; Peterca, M.; Wagner, M.; Obata, M.; Mitchell, C. M.; Cho, W. D.; Balagurusamy, V. S. K.; Heiney, P. A. *J. Am. Chem. Soc.* **2005**, *127*, 15257. (b) Percec, V.; Rudick, J. G. *Macromolecules* **2005**, *38*, 7241.

(15) Tang, B. Z.; Kong, X.; Wan, X.; Peng, H.; Lam, W. Y.; Feng, X.-D.; Kwok, H. S. *Macromolecules* **1998**, *31*, 2419.

(16) (a) Sedlacek, J.; Vohlidal, J. *Collect. Czech. Chem. Commun.* **2003**, *68*, 1745. (b) Schenning, A. P. H. J.; Fransen, M.; Meijer, E. W. *Macromol. Rapid Commun.* **2002**, *23*, 266. (c) Mitsuyama, M.; Kondo, K. *Macromol. Chem. Phys.* **2000**, *201*, 1613. (d) Balcar, H.; Sedlacek, J.; Vohlidal, J.; Zednik, J.; Blechta, V. *Macromol. Chem. Phys.* **1999**, *200*, 2591. (e) Hirao, K.; Ishii, Y.; Terao, T.; Kishimoto, Y.; Miyatake, T.; Ikariya, T.; Noyori, R. *Macromolecules* **1998**, *31*, 3405. (f) Russo, M. V.; Iucci, G.; Furlani, A.; Camus, A.; Marsich, N. *Appl. Organomet. Chem.* **1992**, *6*, 517. (g) Yang, W.; Tabata, M.; Kobayashi, S.; Yokota, K.; Shimizu, A. *Polym. J.* **1991**, *23*, 1135.

(17) Silverstein, R. M.; Bassler, G. C.; Morrill, T. C. *Spectrometric Identification of Organic Compounds*, 5th ed.; Wiley: New York, 1991.

(18) (a) Ito, T.; Shirakawa, H.; Ikeda, S. *J. Polym. Sci., Polym. Chem. Ed.* **1975**, *13*, 1934. (b) Masuda, T.; Tang, B. Z.; Tanaka, T.; Higashimura, T. *Macromolecules* **1986**, *19*, 1459.

(19) (a) Hawker, C. J. *Adv. Polym. Sci.* **1999**, *147*, 113. (b) Cornelissen, J. J. L. M.; Peeters, E.; Janssen, R. A. J.; Meijer, E. W. *Acta Polym.* **1998**, *49*, 471. (c) Chen, J.; Xie, Z.; Lam, J. W. Y.; Law, C. C. W.; Tang, B. Z. *Macromolecules* **2003**, *36*, 1108. (e) Tang, B. Z.; Poon, W. H.; Peng, H.; Wong, H. N. C.; Ye, X.; Monde, T. *Chin. J. Polym. Sci.* **1999**, *17*, 81.

(20) (a) Mayer, S.; Zentel, R. *Prog. Polym. Sci.* **2001**, *26*, 1973. (b) Teramoto, A. *Prog. Polym. Sci.* **2001**, *26*, 667. (c) Shinohara, K.; Yasuda, S.; Kato, G.; Fujita, M.; Shigekawa, H. *J. Am. Chem. Soc.* **2001**, *123*, 3619. (d) Ando, H.; Yoshizaki, T.; Aoki, A.; Yamakawa, H. *Macromolecules* **1997**, *30*, 6199. (e) Tang, B. Z.; Wan, X.; Kwok, H. S. *Eur. Polym. J.* **1998**, *34*, 341.

(21) *Circular Dichroism: Principles and Applications*; Nakanishi, K., Berova, N., Woody, R. W., Eds.; Wiley-VCH: New York, 2000.

(22) Yasugi, K.; Nakamura, T.; Nagasaki, Y.; Kato, M.; Kataoka, K. *Macromolecules* **1999**, *32*, 8024.

(23) (a) Cheuk, K. K. L.; Li, B. S.; Chen, J.; Xie, Y.; Tang, B. Z. *Proc. 5th Asian Symp. Biomed. Mater.* **2001**, 514−518. (b) Tang, B. Z. *Polym. Prepr.* **2002**, *43* (1), 48. (c) Li, B. S.; Cheuk, K. K. L.; Zhou, J.; Xie, Y.; Tang, B. Z. *Polym. Mater. Sci. Eng.* **2001**, *85*, 401.

(24) (a) Nicolini, C. *Molecular Bioelectronics*; World Scientific: Hong Kong, 1996. (b) Lesk, A. M. *Introduction to Bioinformatics*; Oxford University Press: Oxford, England, 2002.

MA062629D